COMPLEXITY ANALYSIS OF SYSTEMATIC SPECTRUM SENSING FOR COGNITIVE RADIO

Jui-Chieh Lin[1], Ming-Jung Fan-Chiang[1], Sao-Jie Chen[1], *Senior Member, IEEE*
([1]Graduate Institute of Electronics Engineering, National Taiwan University, Taipei, Taiwan)
Michael Schulte[2] and Yu Hen Hu[2], *Fellow, IEEE*
([2]Department of Electrical and Computer Engineering, University of Wisconsin – Madison, Madison, USA)

ABSTRACT

Over time, sensing techniques have evolved to achieve higher accuracy and obtain more information. *Systematic spectrum sensing* approaches, which employ a combination of different ad-hoc spectrum sensing techniques, have recently been proposed. Our work explores the implementation of *systematic spectrum sensing* approaches. In this work, three state-of-the-art ad-hoc spectrum sensing techniques, namely, *energy detection*, *cyclic prefix detection*, and the *spectral correlation function* (SCF), are adopted. The spectrum sensing techniques are implemented in ANSI C. Simulation of the *systematic spectrum sensing* approach is performed on the Texas Instrument c6416 Code Composition Simulator. Time-complexity of the *systematic spectrum sensing* approach is discussed.

1. INTRODUCTION

Next generation wireless communication systems are expected to have very high throughput requirements [1]. However, the scarcity of the frequency spectrum may be a major obstacle in the evolution of wireless communication systems. According to a report of the Federal Communications Commission (FCC) in 2002 [2], many licensed spectrums are underutilized in time and frequency— the utilization rates of these licensed spectrums were less than 15%. A possible solution is to share the licensed frequency spectrums, under acceptable inconvenience brought to the licensee, when the frequency bands are vacant. By sharing these underused frequency spectrums, the overall spectrum utilization rate may be improved.

In 1999, Mitola [3][4] proposed the idea of the cognitive radio (CR), which is a promising technology to achieve efficient spectrum utilization. CR is more flexible and intelligent than traditional wireless communication techniques. Conventional radios usually support a fixed standard and rarely switch to other standards. Cognitive radios, in contrast, have the ability to sense their operating environment and can automatically switch between different standards. Cognitive radio is also able to alter the communication parameters, such as modulation type, carrier frequency, bandwidth, and transmission power to optimize the spectrum usage.

In CR systems, the licensees are often referred to as primary users (PUs) and the unlicensed CR users are often referred to as secondary users (SUs). The SUs can only connect via the licensed bands when the bands are not occupied by PUs at particular time slots and around specific geographic locations. Therefore, the SUs must perform spectrum sensing to detect the spectrum holes and verify that PU is absent before access. The SUs are also responsible for vacating the licensed spectrum instantly when the primary users try to access the same spectrum to avoid collisions. Consequently, the SUs shall perform periodic spectrum sensing to detect the presence of the primary users. A spectrum sensing scheme directly impacts the spectrum utilization by reducing the interference rationed to primary users. Therefore, spectrum sensing has become a crucial issue for cognitive radio.

Conventional ad-hoc spectrum sensing techniques, such as *energy detection*, *cyclic prefix detection*, and the *spectral correlation function* (*SCF*) *detection* have been widely investigated and their implementations have been studied [5][6]. Along with the evolution of cognitive radio technology, more accurate sensing algorithms, including *systematic spectrum sensing*, were proposed [7]. Since there has not yet been research on the implementation and complexity of the *systematic spectrum sensing* approach for multi-standard cognitive radio, our work provides an implementation survey of this algorithm.

2. SPECTRUM SENSING SCENARIOS

In this work, we mainly focus on sensing the OFDM-based system due to its widespread access. The system is defined to sense the resources and identifies the activities happening at the bands of interest. The transmission will take place after the resources are allocated. The sensing scenarios are specified in: 802.11a/b/g/n [8-12], 802.16d (Fixed WiMAX) [13] and 802.16e (Mobile WiMAX) [14]. We assume the secondary users and their base station, accessing the medium resource at a lower priority, operate at the same frequency range and communicate in the standards similar to their primary counterparts.

An 802.11b/g system has 14 channels in the 2.4 GHz band, each 5 MHz wide. 802.11a operates using 5.15–5.25, 5.25–5.35 and 5.725–5.825 GHz unlicensed national information structure (U-NII) bands. 802.11a has 12 non-overlapping channels. Operating channels in 802.11a are 20 MHz wide. 802.11n operates in the same frequency band as 802.11a. It can achieve higher data rates because of its provision to use double-width 40 MHz channels.

From a global perspective, the 2.3 GHz, 2.5 GHz, 3.5 GHz, and 5.7 GHz bands will most likely be used for WiMAX deployments. The WiMAX Forum has identified these bands for initial interoperability certifications. In Fixed WiMAX, the 3.5 MHz mode operates at 3.5 GHz and the 10 MHz mode operates at 5.7 GHz, with 56 and 9 channels respectively. In Mobile WiMAX, the 5 MHz mode operates at 2.3 GHz, 2.5 GHz, and 3.5 GHz with 4, 37, and 39 channels respectively.

Figure 1 shows the frequency spectrums used by the wireless communication standards discussed previously.

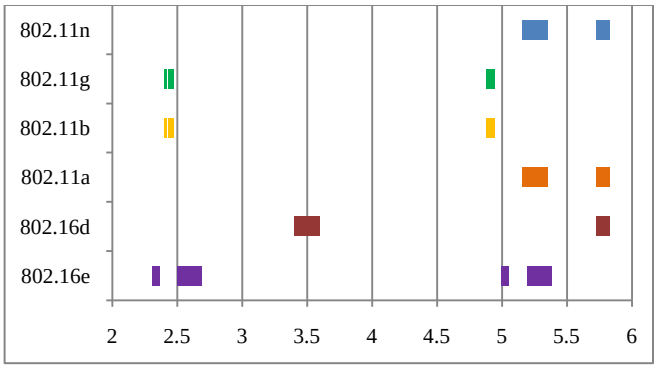

Fig 1. Frequency Spectrum Usage for Targeted Standards.

3. SPECTRUM SENSING TECHNIQUES

In this section, we briefly introduce the adopted ad-hoc techniques for the *systematic spectrum sensing* mechanism.

3.1. Received Signal Strength Indicator (*RSSI*)

A straightforward approach to detect the existence of a single primary user is to measure the received signal energy. Such a process, known as the *received signal strength indicator* (*RSSI*), does not necessarily require receiver synchronization. *RSSI* offers a reasonably reliable channel strength assessment even at low signal levels [15]. It can be shown that the optimal detector is the energy detector [16]:

$$RSSI(r) = \frac{1}{L}\sum_{t=0}^{L-1}\left(\sum_{n=0}^{N-1}\left|r(n)\right|^2\right) \geq \tau_{RSSI} \qquad (1),$$

where $r(n)$ is the complex input signal, L is the observation period, N is length of the observation period, and τ is a pre-determined threshold. A narrowband band pass filter (NB BPF) with central frequency at $1/T_s$, reciprocal of fundamental symbol rate, is employed. The block diagram of the *RSSI* detector is shown in Fig. 2, based on (1).

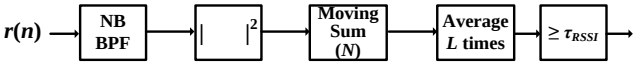

Fig. 2. Block diagram of the RSSI detector.

3.2. Cyclic Prefix Detection (*CP*)

A positive RSSI result is not sufficient to determine a PU exists since the detected energy may come from interference or other users from different standards at the same bands. Therefore, classification of signals by other intrinsic properties is required. By adopting *cyclic prefix* (*CP*) mechanism, the *spectrum sensing system* can determine the existence of an active primary OFDM system in the selected frequency sub-band.

The main problem that wireless receivers cope with is inter-symbol interference (ISI), which results from different delays in different channel. Moreover, since OFDM systems use multiple subcarriers of different frequencies and the subcarriers are packed tightly into an operating channel, small shifts in subcarrier frequencies may cause interference between carriers, a phenomenon called inter-carrier interference (ICI).

Cyclic prefix is one way to implement the *guard interval* (*GI*) to ensure distinct transmissions do not interfere with each other. A period, equal to the length of *guard interval*, of sub-carriers from the tail of the original frame is inserted in front of the frame. Extending each subcarrier does not affect the subcarrier frequencies and therefore ICI is avoided. The *guard interval* with the extended prefix is called the *cyclic prefix* (*CP*).

We follow [7] and [17] for our initial setup. The receiver collects $2N_{FFT} + N_{CP}$ samples at the sampling rate $1/T_s$. It is assumed that the sampled region contains one complete OFDMA symbol [17].

We follow the assumption that the synchronization has not been performed during spectrum sensing. Therefore, parameters such as timing offset and frequency offset denoted as θ and ε respectively, are unknown.

Let I and $\tilde{I}$ be two sampling intervals with *CP* samples, where I contains the cyclic prefix and $\tilde{I}$ contains its replica.

$$I = \{\theta, \theta+1, ..., \theta+N_{CP}-1\}$$
$$\tilde{I} = \{\theta+N_{FFT}, \theta+N_{FFT}+1, ..., \theta+N_B-1\} \qquad (2)$$

The observation space is illustrated in Fig. 3.

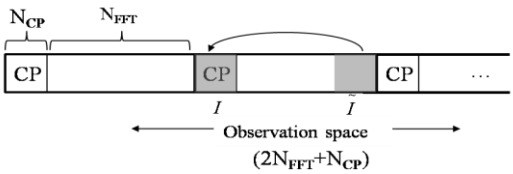

Fig. 3. Observation Space for Detecting *CP*.

If the primary system is active, the samples in the *CP* and its replica are correlated [17]. The likelihood ratio test $M(r)$ is:

$$M(r) = |S(\theta)|\cos(2\pi\varepsilon + \angle S(\theta)) - \lambda P(\theta) \geq \tau_{CP} \quad (3)$$

where

$$S(\theta) = \sum_{n=\theta}^{\theta+N_{CP}-1} r(n)r^*(n+N_{FFT})$$

$$P(\theta) = \sum_{n=\theta}^{\theta+N_{CP}-1} [|r(n)|^2 + |r(n+N_{FFT})|^2]$$

$$\lambda = \frac{SNR}{2(SNR+1)} = \frac{\rho}{2} \text{ ,and } SNR = \frac{\sigma_s^2}{\sigma_w^2}$$

Following the method proposed in [17], a generalized likelihood ratio test can be adopted to estimate the unknown parameters under the maximum likelihood (ML) criterion. Based on the estimated parameters, the likelihood ratio test can be applied. In [17], an ML estimation of timing offset and frequency offset in OFDM systems is specified as:

$$M(r) = \underset{0\leq\theta\leq N_{FFT}}{Max} \{|S(\theta)| - \lambda P(\theta)\} \geq \tau_{CP} \quad (4)$$

The simulation in [7] showed that *CP* detection reached 95% accuracy when the observation period was 4 symbols. The resulting block diagram is presented in Fig. 4.

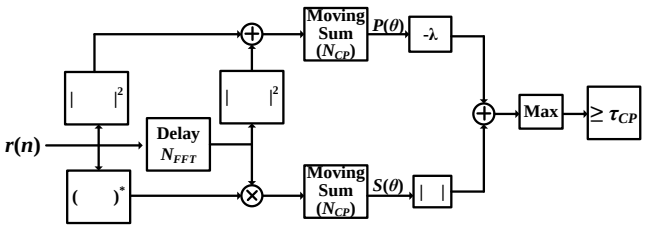

Fig. 4. Block Diagram of a CP Detector with Known Total Power and SNR.

3.3. Spectral Correlation Function (*SCF*) Detection

Many communication signals nowadays exhibit embedded periodicity, such as sinusoidal carriers and pulse trains, and can be modeled as cyclostationary signals. The embedded cyclostationary feature occurs in the spectrum and can be analyzed using the *spectral correlation function* (*SCF*) [18]:

$$S_x^\alpha(f) = \lim_{\substack{\Delta f\to\infty \\ \Delta t\to\infty}} \frac{1}{\Delta t}\int_{\frac{-\Delta t}{2}}^{\frac{\Delta t}{2}} \Delta f X_{\frac{1}{\Delta f}}(t, f+\frac{\alpha}{2}) X^*_{\frac{1}{\Delta f}}(t, f-\frac{\alpha}{2})dt \quad (5)$$

where

$$X_{1/\Delta f}(t,v) = \int_{t-1/2\Delta f}^{t+1/2\Delta f} x(u)e^{-i2\pi vu}du$$

denotes the complex envelope of the narrow-band component of $x(t)$ with bandwidth Δf at center frequency v. Following [19], we embed the signature generation and analysis scheme and adopt a time-smoothed cyclic cross periodogram [20]:

$$\hat{S}_x^\alpha[k] = \frac{1}{L}\sum_{t=0}^{L-1} X[k]X^*[k-\alpha]W[k] \quad (6)$$

where $W[k]$ is defined as a smoothing spectral window and $X[k]$ as the Fourier transform of the received signal $x[n]$:

$$X[k] = \sum_{n=0}^{N-1} x[n]e^{-i2\pi nk/N}$$

.

The length of the window equals OFDM symbol length N while L windows are involved. By estimating the cyclic cross spectrum at a range of cyclic frequencies, the *SCF* is obtained. The method is estimator for cyclic cross spectrum was shown to be consistent, asymptotically unbiased, and complex normally distributed [20].

Let $\tilde{S}_x^\alpha(f)$ be the output of cyclic periodogram passing through notch filter, the optimum feature detection correlates the cyclic periodogram with the ideal spectral correlation function as [19]:

$$y_\alpha(t) = \int_{-\infty}^{\infty} S_s^\alpha(f) * \tilde{S}_x^\alpha(f)dfe^{i2\alpha\pi t} \quad (7)$$

In OFDM systems, the spectral resolution Δf equal subcarrier spacing, (9) can be approximated with a rectangular window— $W[k]$ of width $M\Delta f$, where M is the number of subcarriers mapped. Consequently, the signature detector can be implemented as:

$$y_\alpha = \underset{m}{Max}\sum_{k=0}^{K-1} \hat{S}_x^\alpha[k]W[m-k] \quad (8)$$

The *SCF* method requires enough observation time to reduce the random effects generated by the smoothing method. The experiment results in [19] showed that the *SCF* signature detection reached 100% accuracy when the observation period was 60 symbols. Since the algorithm adopts the Fourier transform, it may be accelerated by the FFT hardware supported in OFDM receivers. Fig. 5 shows the block diagram of the SCF detector unit.

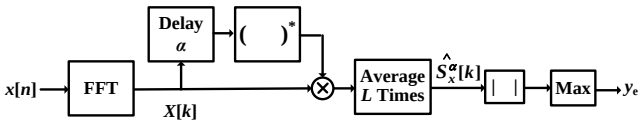

Fig. 5. Block diagram of SCF detector

4. SPECTRUM SENSING STRATEGY

In this section, we describe our methodology for detection of spectrum utilization. The methodology is applicable to different sensing scenarios, even though the particular sensing techniques adopted may change.

We divide the operating spectrum into four intervals and classify them into three cases, as shown in Fig. 6. Intervals (a) and (c) are classified under first case, which is a single standard case. The second case is in interval (b), in which there are two standard systems; one is OFDM-based the other is not. The last case, in interval (d), is the most complex situation because three OFDM-based standard systems operate in this interval.

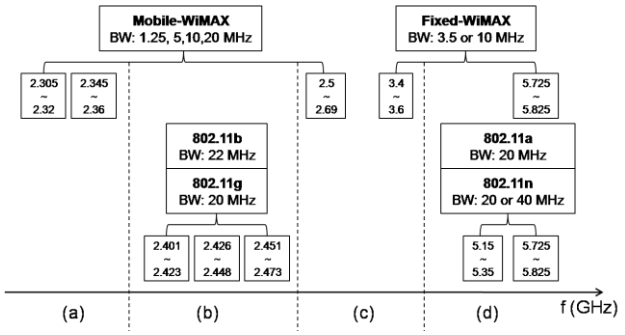

Fig 6. Categories of Spectrum Sensing Mechanisms.

Multiple primary users' detection and differentiation is an important issue in multi-standard spectrum sensing. We analyze the signal properties in our scenario and propose appropriate sensing techniques based on features of the signal.

When CR operates in a single PU case, we can just choose the simplest *received signal strength indicator* (*RSSI*) mechanism to detect whether the PU exists or not. But when CR operates in a multi-standard scenario, the RSSI mechanism is not enough because it cannot distinguish different PUs.

In case two, the PU signals from the two standards can be separated by OFDM feature detection. Taking computation complexity into consideration, time-domain features detection is better than frequency-domain detection, because frequency-domain detection always needs an FFT function to translate signals from the time domain to the frequency domain. Therefore, in this case, we choose the time-domain feature as the *CP* to detect and distinguish the PUs.

In case three, the PU signals from the three standards are all OFDM-based. Since the *CP* lengths defined are different in each standard, the minor differences between the *CP* lengths may reduce the accuracy of detection. Therefore, we draw support from other features, such as *SCF*.

5. SIMULATION RESULTS

In this section, we focus on the execution time performance of the proposed spectrum sensing code on a DSP platform.

5.1. Execution Cycles of the Original Programs

We assume that multiple standards coexist in the scenario. Table 1 shows the standards' relevant parameters in the OFDM-based systems. Table 2 shows the execution cycles of the three detector functions using the Texas Instrument C64 Code Composer Studio (CCS) Emulator. We convert the execution cycles into execution times on a TI C64 DSP with a 600 MHz clock frequency, and the performance in μs is presented in Table 3 These results are for C code implementations written in fixed-point using a16-bit data format.

Table 1. Parameters in OFDM-based systems.

	FFT/data (samples)	CP (ratio/samples)	GI Duration	Symbol Duration
802.11a/g	64/48	1/4 (16)	0.8us	4us
802.11n	64/52	1/4 (16)	0.8us	4us
		1/8 (8)	0.4us	3.6us
	128/108	1/4 (32)	0.8us	4us
		1/8 (16)	0.4us	3.6us
802.16d	256/192	1/8 (32)	8us	72us
802.16e	512/360	1/8 (64)	11.4us	102.9us

Table 2. General C Code's Execution Cycles.

	RSSI	CP	SCF
802.11a/g	2849	477856	2253203
802.11n	2849	477856	2253203
		254604	
	5665	1823528	4966612
		946980	
Fixed WiMAX	11297	3646584	10376996
Mobile WiMAX	22561	14305068	22708023

Table 3. Execution Time (TI C64 @600 MHz).

	RSSI(μs)	CP(μs)	SCF(μs)
802.11a/g	4.76	798.02	3762.85
802.11n	4.76	798.02	3762.85
		425.2	
	9.46	3045.3	8294.24
		1581.46	
802.16d	18.866	6089.8	17329.6
802.16e	37.68	23889.5	37922.4

5.2. Texas Instrument C6416 Related Optimization

The TI C6416 DSP supports 32-bit and 16-bit words, which are denoted as integer-word and short-word, respectively. C6416 also provides intrinsic instructions to optimize data flow bandwidth, such as packing two short-words into one integer-word, and therefore double the

effective bandwidth. For a memory access intrinsic like "_amem4" (which allows aligned loads and stores of 4 bytes to memory.), we have to use corresponding intrinsics to perform operations, such as "_add2" (which adds the upper and lower halves of src1 to the upper and lower halves of src2 and returns the result. Any overflow from the lower half addition does not affect the upper half addition), "_mpy" (which multiplies the 16 LSBs of src1 by the 16 LSBs of src2 and returns the result), and "_mpyh" (which multiplies the 16 MSBs of src1 by the 16 MSBs of src2 and returns the result) [21]. There are many intrinsic that operate on 16-bit data, because this data type provides the most efficient use of the 16-bit multiplier in the C6416. Therefore, we choose the "short" data type and use the related intrinsics to enhance the execution performance. It is worth mentioning that loop unrolling techniques are essential when the data flow bandwidth is changed.

We also adopt the C64x DSPLIB that consists of assembly-optimized signal-processing routines [21]. The identified signal processing operations in our spectrum sensing process are "*sum of square*", "*correlation*" and "*FFT*". The sum of square operation does not have a matching library call. It is implemented with the *multiply-and-add* function with both inputs of the multiplier the same. Therefore, using TI-intrinsic to implement *Cyclic Prefix sensing*, in which *Sum-of-Square* is the major operation, outperforms DSP Library.

The optimization level was set as opt-2 in the compiler's option. Software pipelining optimization is enabled to improve the performance of the for-loop [22].

Table 4. RSSI Execution Cycles for Different Codes.

	General C	TI-Intrinsic	Call DSPLib -o2
802.11a/g	2849	2209	103
802.11n	2849	2209	103
	5665	4353	135
802.16d	11297	8641	199
802.16e	22561	17217	327

Table 5. CP Execution Cycles for Different Codes.

	General C –o2	Intrinsic -o2	Call DSPLib -o2
802.11a/g	70844	21396	24124
802.11n	70844	21396	24124
	67152	20684	23620
	140556	28312	32640
	134152	28020	32512
802.16d	268380	41368	49408
802.16e	536848	68584	81752

Table 6. SCF Execution Cycles for Different Codes.

	General C –o2	Intrinsic -o2	Call DSPLib -o2
802.11a/g	281537	957899	78621
802.11n	281537	957899	78621
	637183	1926203	168205
802.16d	1228397	3841211	325773
802.16e	2810231	7685228	718972

5.3 Overall Performance

Table 7 lists the execution cycles of each three detector function after optimization. Table 8 shows the corresponding execution times assuming that the clock frequency of the DSP is 600 MHz. Since the results presented in Tables 1 to 6 are for sensing a respective single channel, the number of channels supported by the standards should be considered.

For intervals (a) and (c), we use the RSSI detector to sense the existence of a single primary user. The execution time is:

$$0.546\times 4+0.546\times 37+0.332\times 56=40.978(us).$$

For interval (b) in case-2, the CP detector is employed to separate between OFDM 802.11g and non-OFDM 802.11b. The execution time is calculated as:

$$(0.172+35.73)\times 14=502.628(us).$$

Finally, for interval (d), which is the most complex, the SCF detector is executed three times for three different bandwidths. The execution time is calculated as:

$$(0.332+406.24)\times 9+(0.225+107.34)\times 12+(0.172+213.85)\times 6 = 6233.742(us).$$

Consequently, performing the *systematic spectrum sensing* for the most complicated band under our scenario takes 6777.348μs, or approximately 7ms.

A summary of the number of symbols required to meet the accuracy requirements is listed in Table 9. It can be observed that the *RSSI* and *SCF* detectors have less processing time than the required data duration. Therefore, future DSPs employing these two algorithms can operate at lower speeds. For the CP, however, the processing time is slower than the speed of input streaming data. Since the spectrum sensing is not real-time processing, the latency does not cause problems for spectrum sensing. The results indicate that future spectrum sensing implementations may need to focus on CP to enable faster sensing, which may help lead to better cognitive ability.

Table 7. Execution Cycles of Spectrum Sensing Functions.

	RSSI	CP	SCF
802.11a/g	103	21396	64276
802.11n	103	21396	64276
		20684	
	135	28312	128056
		28020	
802.16d	199	41368	243256
802.16e	327	68584	514134

Table 8. Execution Time of Spectrum Sensing Functions. (@600 MHz)

	RSSI(μs)	CP(μs)	SCF(μs)
802.11a/g	0.172	35.73	107.34
802.11n	0.172	35.73	107.34
		34.54	
	0.225	47.3	213.85
		46.8	
802.16d	0.332	69.1	406.24
802.16e	0.546	114.54	858.6

Table 9. Number of Symbols to Meet Accuracy Requirements.

Symbols Required	RSSI	CP	SCF
	1	4	60
Effective Time	**RSSI(μs)**	**CP(μs)**	**SCF(μs)**
802.11a/g	4	16	240
802.11n	4	16	240
	3.6	14.4	216
	4	16	240
802.16d	72	288	4320
802.16e	102.9	411.6	6174

6. CONCLUSIONS

In this work, we proposed a methodology to perform multi-standard spectrum sensing. By analyzing the overlap of the operating frequencies for different standards, we propose a spectrum sensing mechanism, including received signal strength indicator (RSSI), cyclic prefix (CP) detection, and spectral correlation function (SCF), to detect 802.11a/b/g/n, Fixed WiMAX and Mobile WiMAX. The complexity analyses among these ad-hoc sensing mechanisms are performed. The spectrum sensing program takes 7ms on a 600MHz sense the spectrums containing 802.11a/b/g/n, Fixed WiMAX and Mobile WiMAX standards on a TI TMS320C6416 DSP running at 600MHz. The most cycle consuming operations are *sum of squares operations.* Our simulation results indicate a future spectrum sensing accelerator may be architecture similar to TI TMS320C6416 DSP and operates at 41.9 MHz, given an assumed updating period of 0.1 seconds. Moreover, a fast *sum-of-squares* hardware can greatly increase the efficiency of such an accelerator.

REFERENCES

[1] J. Z. Sun, J. Sauvola, and D. Howie, "Features in future: 4G visions from a technical perspective," in *Proc. 2001 IEEE Global Telecommun. Conf.* (*GLOBECOM '01*), Nov. 2001, pp. 3533-3537.

[2] Federal Communications Commission (FCC), "Spectrum policy task force," *ET Docket no. 02-135*, Nov. 15, 2002.

[3] J. Mitola III and G. Q. Maguire, Jr., "Cognitive radio: Making software radios more personal," *IEEE Pers. Commun*., vol.6, no. 4,pp. 13-18, Aug. 1999.

[4] J. Mitola, "Cognitive Radio: An integrated agent architecture for software defined radio," *PhD dissertation*, Royal Institute of Technology (KTH), Sweden, 2000.

[5] D.Cabric, S. M. Mishra, R.B. Brodersen, "Implementation Issues in Spectrum Sensing for Cognitive Radios", *38th Annual Asilomar Conference on Signals,Systems and Computers*, November 2004.

[6] W.A.Gardner, "Signal Interception: A Unifying Theoretical Framework for Feature Detection", *IEEE Trans. on Communications*, vol. 36, no. 8. August 1988.

[7] S.-Y. Tu, K.-C. Chen, and R. Prasad, "Spectrum sensing of OFDMA systems for cognitive radio networks", *IEEE Trans. Veh. Technol.*, vol. 58, no. 7, pp. 3410–3425, Sep. 2009.

[8] IEEE Standard 802.11-1999. Part 11: Wireless LAN Medium Access Control (MAC) and Physical Layer (PHY) specifications, Aug. 1999.

[9] IEEE Standard 802.11b-1999 (R2003). Part 11: Wireless LAN Medium Access Control (MAC) and Physical Layer (PHY) specifications—High-speed Physical Layer in the 5 GHz Band, Jun. 2003.

[10] IEEE Standard 802.11a-1999 (R2003). Part 11: Wireless LAN Medium Access Control (MAC) and Physical Layer (PHY) specifications—Higher-Speed Physical Layer Extension in the 2.4 GHz Band, Jun. 2003.

[11] IEEE Standard 802.11g-2003. Part 11: Wireless LAN Medium Access Control (MAC) and Physical Layer (PHY) specifications—Amendment 4: Further Higher Data Rate Extension in the 2.4 GHz Band, Jun. 2003.

[12] IEEE Standard 802.11n-2009. Part 11: Wireless LAN Medium Access Control (MAC) and Physical Layer (PHY) specifications—Amendment 5: Enhancements for Higher Throughput, Oct. 2009.

[13] IEEE Standard 802.16-2004. Part16: Air interface for fixed broadband wireless access systems, Oct. 2004.

[14] IEEE Standard 802.16e-2005. Part16: Air interface for fixed and mobile broadband wireless access systems—Amendment for physical and medium access control layers for combined fixed and mobile operation in licensed band, Dec. 2005.

[15] IEEE Standard for Local and Metropolitan Area Networks Part 16: Air Interface for Fixed Broadband Wireless Access Systems, Mar. 2004.

[16] M. Oerder, and H. Meyr, "Digital filter and square timing recovery," *IEEE Trans. Communications*, vol. 36, May 1988.

[17] J. J. van de Beek, M. Sandell, and P. O. Borjesson, "ML estimation of timing and frequency offset in OFDM systems," *IEEE Trans. Signal Processing*, vol. 45, pp. 1800-1805, Jul. 1997.

[18] W. Gardner, "Signal interception: a unifying theoretical framework for feature detection," *IEEE Trans. Commun.*, vol. 36(8), pp. 897–906, 1988.

[19] P. D. Sutton, K. E. Nolan, and L. E. Doyle "Cyclostationary signatures in practical cognitive radio applications," *IEEE Journal of Selected Area and Communications*, vol. 26, no. 1, Jan. 2008.

[20] B. Sadler and A. Dandawate, "Nonparametric estimation of the cyclic cross spectrum," *Information Theory, IEEE Transactions on*, vol. 44, no. 1, pp. 351–358, 1998.

[21] Texas Instruments, TMS320C64x DSP Library Programmer's Reference, *SPRU565B*, Oct.2003.

[22] Texas Instruments, TMS320C6000 Programmer's Guide, *SPRU198G, Oct.2002*.